AD-A159 895 X-RAY SCATTERING FROM POLY(THIOPHENE): CRYSTALLINITY AND CRYSTOLLOGRAPHY. (U) CALIFORNIA UNIV SANTA BARBARA INST FOR POLYMERS AND ORGANIC S... Z MO ET AL. 1/1

UNCLASSIFIED 01 OCT 85 IPOS-ONR-7 N00014-83-K-0450 F/G 20/2 NL

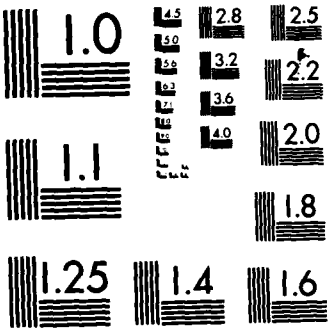

OFFICE OF NAVAL RESEARCH

Contract N00014-83-K-0450

Technical Report No.7

X-Ray Scattering from Poly(thiophene): Crystallinity and Crystallography Structure

To be Published in Macromolecules

by

Z. Mo, K.-B. Lee, Y. B. Moon, M. Kobayashi, A. J. Heeger and F. Wudl

Institute for Polymers and Organic Solids
Department of Physics
University of California, Santa Barbara
Santa Barbara, CA 93106

SECURITY CLASSIFICATION OF THIS PAGE

REPORT DOCUMENTATION PAGE

1a. REPORT SECURITY CLASSIFICATION: NONE	1b. RESTRICTIVE MARKINGS: NONE
2a. SECURITY CLASSIFICATION AUTHORITY: NONE	3. DISTRIBUTION/AVAILABILITY OF REPORT: Unlimited
2b. DECLASSIFICATION/DOWNGRADING SCHEDULE: NONE	
4. PERFORMING ORGANIZATION REPORT NUMBER(S): IPOS - ONR # 7	5. MONITORING ORGANIZATION REPORT NUMBER(S): ONR N00014-83-K-0450
6a. NAME OF PERFORMING ORGANIZATION: University of California Santa Barbara, CA 93106 / 6b. OFFICE SYMBOL (If applicable)	7a. NAME OF MONITORING ORGANIZATION: Offive of Naval Research
6c. ADDRESS (City, State and ZIP Code): Santa Barbara, CA 93106	7b. ADDRESS (City, State and ZIP Code): 800 North Quincy Avenue Arlington, VA 22217
8a. NAME OF FUNDING/SPONSORING ORGANIZATION: Office of Naval Research / 8b. OFFICE SYMBOL (If applicable)	9. PROCUREMENT INSTRUMENT IDENTIFICATION NUMBER
8c. ADDRESS (City, State and ZIP Code): 800 N. Quincy Avenue Arlington, VA 22217	10. SOURCE OF FUNDING NOS. — PROGRAM ELEMENT NO.: - / PROJECT NO.: - / TASK NO.: - / WORK UNIT NO.: -
11. TITLE (Include Security Classification): "X-Ray Scattering from Poly(thiophene): Crystallinity & Crystollography Structure"	
12. PERSONAL AUTHOR(S): Z. Mo, K.-B. Lee, Y. B. Moon, M. Kobayashi, A. J. Heeger and F. Wudl	
13a. TYPE OF REPORT: Technical / 13b. TIME COVERED: FROM _____ TO _____	14. DATE OF REPORT (Yr., Mo., Day): 10/1/85 / 15. PAGE COUNT
16. SUPPLEMENTARY NOTATION: None	
17. COSATI CODES — FIELD / GROUP / SUB. GR	18. SUBJECT TERMS (Continue on reverse if necessary and identify by block number)

19. ABSTRACT (Continue on reverse if necessary and identify by block number)

X-ray scattering has been used to investigate the crystallinity and crystal structure o chemically coupled polythiophene. Heat treatment at elevated temperatures leads to significant increases in crystallinity (from ~ 35% as-synthesized up to ~ 56% after annealing at 380°C for 30 minutes) and coherence length indicative of chain growth and extension. Chemical analysis of the chain extended PT shows a major reduction in residual iodine content consistent with growth of the polymer chains to approximately 1200 thiophene rings. An initial model of the crystal structure of polythiophene is presented.

20. DISTRIBUTION/AVAILABILITY OF ABSTRACT: UNCLASSIFIED/UNLIMITED ☒ SAME AS RPT ☐ OTIC USERS ☐	21. ABSTRACT SECURITY CLASSIFICATION: None
22a. NAME OF RESPONSIBLE INDIVIDUAL: Alan J. Heeger	22b. TELEPHONE NUMBER (Include Area Code): (805) 961-3184 / 22c. OFFICE SYMBOL

DD FORM 1473, 83 APR EDITION OF 1 JAN 73 IS OBSOLETE.

SECURITY CLASSIFICATION OF THIS PAGE

X-Ray Scattering from Poly(thiophene): Crystallinity and Crystollographic Structure

Z. Mo, K.-B. Lee, Y.B. Moon, M. Kobayashi,
A.J. Heeger and F. Wudl

Institute for Polymers and Organic Solids
Department of Physics
University of California
Santa Barbara, CA

Abstract

X-ray scattering has been used to investigate the crystallinity and crystal structure of chemically coupled polythiophene. Heat treatment at elevated temperatures leads to significant increases in crystallinity (from ~ 35% as-synthesized up to ~ 56% after annealing at 380°C for 30 minutes) and coherence length indicative of chain growth and extension. Chemical analysis of the chain extended PT shows a major reduction in residual iodine content consistent with growth of the polymer chains to approximately 1200 thiophene rings. An initial model of the crystal structure of polythiophene is presented.

1. Introduction

Polythiophene (PT) can be viewed as an sp^2p_z carbon chain in a structure (see Fig. 1) somewhat analogous to that of cis-$(CH)_x$, but stabilized in that structure by the sulfur, which covalently bonds to neighboring carbons to form the heterocycle.[1] Conjugated polymers such as polythiophene are of current interest since they are semiconductors which can be doped with resulting electronic properties that cover the full range from insulator to metal.[2] Moreover, the polyheterocycles are of specific theoretical interest since the two valence bond configurations sketched in Fig. 1(b) are not energetically equivalent.[3] As a result, the inherent coupling of electronic excitations to chain distortions in such linear conjugated polymers leads to the formation of polarons and bipolarons as the dominant species involved in charge storage and charge transport.

High quality polythiophene has recently been synthesized by chemical coupling of 2,5-di-iodothiophene.[1] Based upon chemical analysis of the residual iodine content, the chemically prepared polythiophene consists of polymer chains with approximately 45 thiophene rings (~180 carbon atoms along the backbone). This chemically coupled polythiophene contains a relatively small concentration of unpaired spins and a clean ir spectrum; indicative of a stereoregular polymer with a relatively high degree of structural perfection. Moreover, preliminary x-ray scans showed that the polymer is crystalline.[4]

Photoexcitation of neutral PT leads to photogeneration of polarons with associated changes in the visible-ir absorption spectrum and with photoinduced ESR.[5] In-situ studies[3] of PT during electrochemical doping have demonstrated that in the dilute regime, charge is stored in bipolarons; weakly confined soliton pairs with a confinement parameter $\gamma \cong 0.1\text{-}0.2$. After doping to saturation with AsF_5 (~24 mole%), the electrical conductivity increased by

nearly 10 orders of magnitude[1] to 14 $\Omega^{-1}cm^{-1}$. Moreover, the optical properties,[3] the magnitude and temperature dependence of the thermopower,[1] and the existence of a temperature independent Pauli spin susceptibility[6] all indicate a truly metallic state for the heavily doped polymer.

In this paper, we focus on an x-ray scattering investigation of the crystallinity and crystallographic structure of chemically coupled PT. We find that heat treatment at 300°C for 30 minutes leads to significant increases in crystallinity (from ~35% as-synthesized up to ~52%) and coherence length indicative of chain growth and extension. This is accompanied by loss of iodine; chemical analysis of the chain extended PT shows a major reduction in residual iodine content consistent with growth of polymer chains to approximately 1200 thiophene rings, or a molecular weight of $\sim 10^5$. From analysis of the powder pattern Bragg diffraction, we have obtained crystallographic data which allow indexing and identification of the unit cell parameters. Based upon one-to-one similarities with the d-spacings found for poly(paraphenylene), an initial model of the structure is presented with two polythiophene chains in the unit cell.

II. Experimental Techniques

The polythiophene used in these experiments was synthesized by condensation polymerization of 2,5-di-iodothiophene as described earlier.[1] The composition (as obtained from chemical analysis) of the as-synthesized polymer is given in Table 1. The dark brown powder was packed into an aluminum mold (0.80" x 0.40" x 0.12") for heat treatment and subsequent x-ray scattering measurements.

The x-ray scattering apparatus utilizes a Huber 430/440 goniometer which allows independent horizontal rotations of the sample and the detector with

angular resolution of 0.001°. The Cuk_{α} radiation was provided by a 1 kW Phillips x-ray tube (40 kV at 25 mA). As monochromator and analyzer we used flat HOPG crystals. Powder scans were obtained from the as-synthesized polymer and from the same sample after annealing in dry N_2 at 200°C, 250°C, 300°C, and 380°C for 30 minutes. In a separate series of experiments, the heat treatment was carried out with the sample in air.

III. Experimental Results

The powder pattern scans are plotted in Fig. 2a for a single sample which was heat treated in dry nitrogen. In a separate experiment, a different sample was heat treated at 380°C (Fig. 2b). The solid curves drawn through the data points in Fig. 2 represent a least-squares fitting function composed of a sum of Gaussians. For example, to describe the data after the 300°C anneal, the fitting function consisted of five narrow Gaussian peaks for the sharp Bragg reflections and two broad Gaussians for the diffuse background. These are better resolved in Fig. 2b, where eleven lines can be observed. Thus, the scattered intensity from the crystalline regions, $I_{cr}(\theta)$, is represented by the five narrow Gaussians, whereas the total scattered intensity, $I_t(\theta)$ is represented by the full sum of seven Gaussians. Similar fits were constructed for each data set. Since the fits are in all cases excellent, the fitting functions are used for the quantitative analysis described in the following section. The best fits to the data obtained from the as-synthesized sample and the same sample after the 300°C anneal are compared directly in Fig. 3.

The effects of heat treatment are evident in Figs. 2 and 3:

i) The Bragg peaks are successively narrower after annealing at higher temperatures.

ii) The integrated area under the Bragg peaks increases after annealing at higher temperature.

iii) The diffuse scattering background decreases after annealing at higher temperatures.

We find, furthermore, that the widths of the Bragg peaks are consistently slightly narrower if the sample is cooled slowly subsequent to the anneal (rather than quenched rapidly to room temperature). These changes imply an increase in the volume fraction of the sample which is crystalline and an improvement in the coherence length (i.e. the perfection) of the crystalline regions. Detailed analysis of the data (see following section) confirm the increase in crystallinity and crystallite coherence, and provide quantitative measures of the relevant parameters.

The x-ray data for the strongest crystalline Bragg reflection obtained after annealing N_2 are summarized and compared in Table 2. The three improvements noted above are obtained for samples annealed either in air or in N_2. The excellent stability of polythiophene in air at elevated temperatures is of particular interest.

IV. Ruland Analysis of the Crystallinity

The crystallinity of polythiophene as-synthesized and after heat treatment was determined by the Ruland method.[7,8] The volume fraction of the sample which is crystalline, X_{cr}, is defined as follows:

$$X_{cr} = \frac{\int_0^\infty q^2 I_{cr}(q)\, dq}{K \int_0^\infty q^2 I_t(q)\, dq} \qquad (1)$$

where $I_{cr}(q)$ is the intensity under the Bragg peaks, $I_t(q)$ is the total scattered intensity (Bragg peaks plus diffuse background), and q is the magnitude of the scattering vector, $q = 4\pi \sin\theta/\lambda$. The correction factor, K, is a weighted Debye-Waller factor

$$K = \frac{\int_0^\infty q^2 \langle f^2 \rangle e^{-kq^2} dq}{\int_0^\infty q^2 \langle f^2 \rangle dq} \tag{2}$$

where

$$\langle f^2 \rangle = \Sigma N_i f_i^2 / \Sigma N_i \tag{3}$$

is the weighted mean-square atomic form factor of the polymer; $f_i(q)$ is the form factor of an atom of type i, and N_i is the number of such atoms (per monomer). The imperfection factor, k, arises since thermal motion and lattice imperfection cause part of the x-ray intensity scattered from the crystalline region to appear in the diffuse background.

Equations (1) and (2) give

$$X_c = \left[\frac{\int_0^\infty q^2 I_{cr}(q)\, dq}{\int_0^\infty q^2 I_t(q)\, dq}\right] \left[\frac{\int_0^\infty q^2 \langle f^2 \rangle dq}{\int_0^\infty q^2 \langle f^2 \rangle e^{-kq^2} dq}\right] \tag{4}$$

The finite range in 2θ (and in q) of the experimental data necessarily limit the integration range from 2θ = 7° ($q_1 \cong 0.45 \times 10^8$ cm^{-1}) to 2θ = 60° ($q_{max} \cong 4.1 \times 10^8$ cm^{-1}). Nevertheless, the crystallinity can be estimated with reasonable accuracy by the limited range integrals of eqn. (5):

$$X_{c_r} = K(k)^{-1} \frac{\int_{q_1}^{q_2} q^2 I_{cr}(q)\, dq}{\int_{q_1}^{q_2} q^2 I_t(q)\, dq} \qquad (5)$$

For fixed q_1, if q_2 is large enough, the inferred crystallinity will be independent of q_2. As a procedure, therefore, the best value of X_{cr} is determined by varying the disorder parameter (k) computing X_{cr} as a function of the upper limit (q_2), and finding the value of k which yields a constant X_{cr}; i.e. independent of q_2.

The data of Fig. 2 are replotted as $q^2 I_t(q)$ vs. q in Fig. 4. After correction for polarization, this total intensity was resolved (using the fitting function) into the background diffuse scattering contribution and the crystalline diffraction contribution, $q^2 I_{cr}(q)$. The $q^2 I_t(q)$ plots for the as-synthesized sample and for the same sample after annealing at 300°C are compared directly in Fig. 5. The effect of the heat treatment is clearly evident.

The crystallinity values were obtained through application of eqn. 5; the results are summarized in Table 3. Examination of Table 3 shows that for k = 0.05×10^{-16} to 0.075×10^{-16} cm^2 reasonably constant values are obtained for the crystallinity independent of the upper limit (q_2) of the integral. Although the precise value of X_{cr} depends on the choice of the best k, the trend is clear and unambiguous; the crystallinity increases upon annealing from values of about 35% for the as-synthesized material to values of about 55% after the 300°C anneal. Re-writing the effective Debye-Waller factor as $\exp(-kq^2) \equiv \exp(-1/3\langle u^2\rangle q^2)$, this range of k corresponds to average rms displacements from the perfect lattice (in the crystalline regions) of $\langle u^2\rangle^{1/2} \cong$ 0.3-0.5Å. After the anneal at 380°C, the Ruland analysis yields a value for

$X_{cr} \cong 0.56$ with k somewhat reduced ($k \cong 0.05 \times 10^{-16}$ cm^2) consistent with improved order in the crystalline regions. The coherence length (after 380°C heat treatment) increased to $\xi \cong 174\text{Å}$.

The resulting values for X_{cr} (with $k = 0.076 \times 10^{-16}$ cm^2) are plotted in Fig. 6 as a function of the heat treatment temperature. The annealing procedure causes a clear and unambiguous increase in the crystallinity from $X_{cr} = 0.37$ for the as-synthesized polymer to $X_{cr} = 0.52$ after annealing at 300°C for 30 minutes (either in dry nitrogen or in air). This increase in crystallinity is accompanied by a narrowing of the diffraction peaks and by an increase in the observable number of diffraction peaks. For example, one sees only three Bragg peaks for the as-synthesized polymer, whereas there are five clearly observable Bragg peaks after annealing at 300°C.

The narrowing of the diffraction peaks (see Fig. 2, Fig. 4, and Table 2) implies an incrase in the coherence length (or crystallite size) as a result of the elevated temperature anneal. Assuming all the line broadening results from finite crystallite size The coherence length (in Å) was calculated from the Sherrer equation[9]

$$\xi = 57.3\ \lambda/\beta\cos\theta$$

where $\beta = (B^2-b_0^2)^{\frac{1}{2}}$, B is the measured half-width of the experimental profile (in degrees), b_0 is the instrumental resolution (in degrees), λ is the wavelength of the x-radiation and 2θ is the scattering angle. The instrumental resolution, obtained from scans of single crystal silicon, was found to be 0.2°. Using the data of Table 2 for the strongest crystalline reflection, the calculated coherence length is plotted as a function of annealing temperature in Fig. 7.

The increased crystallinity and crystalline coherence which results from the high temperature heat treatment arises from a combination of two effects; chain extension by oligomer-oligomer reaction and improved chain-chain lateral packing resulting from increased chain mobility at elevated temperatures. The principal evidence indicating chain extension comes from chemical analysis. Evolution of iodine was observed during the annealing period. Since the chemical coupling of 2,5-di-iodothiophene necessarily leaves an iodine atom at the chain end, the iodine content is a direct indicator of molecular weight. To quantify the loss of iodine, the 300°C anneal was repeated for chemical analysis with the sample in dynamic vacuum (the material which evolved was trapped in the vacuum line). The chemical analysis results from the annealed material are included for comparison in Table 1. The residual iodine content decreased from 3.17% (as-synthesized) to 0.13% after heat treatment at 300°C. Assuming all of the residual iodine is covalently bonded at the chain ends, the heat treated polythiophene has undergone significant chain extension to an average of approximately 1200 thiophene rings, or a molecular weight of $\sim 10^5$.

In spite of the significant improvements which result from the highest temperature (380°C) anneal, the resulting polymer is only ≅56% crystalline, and the crystalline regions are imperfect with mean square deviation from the perfect lattice sites of approximately 0.3Å. Thus, although the annealing leads to significant improvement, the resulting polythiophene material is far from the complete ideal crystalline equilibrium. Although exposure to higher temperature for extended periods of time might be expected to lead to further improvement, the onset of polymer degradation sets a practical upper limit of ~380°C (in N_2) as indicated by the thermogravimetric analysis (TGA) data of Fig. 8. The weight loss at 380°C is approximately 7 wt%; i.e. greater than the change in iodine content as determined by elemental analysis. Thus, in

addition to chain extension some evolution of short oligomers must be involved. This was confirmed by analysis of the ir spectrum of the trapped material which showed the presence of thiophene rings.

V. Crystallographic Data: Unit Cell Parameters and Model of the Structure

Table 4 lists the observed d-spacings corresponding to the crystalline reflections of polythiophene. Although the lattice constants cannot be unambiguously determined with these few reflections, we have attempted to index the unit cell using the data from related systems as a guide. The corresponding data[10] from poly(p-phenylene) are therefore listed for comparison in Table 4. The one-to-one correspondence in the observed d-spacings implies a similar crystal structure and similar chain packing for the two systems. This implies an individual chain structure for polythiophene in which the thiophene units alternate as shown in Figure 1. Such an alternating structure is generally accepted for poly(heterocycles) and results in a straight chain conformation. The alternative chain structure (with the rings oriented with sulfur atoms always on one side) would lead to significant curvature of the polymer chain requiring a spiral conformation and a crystal structure very different from that of poly(paraphenylene).

In attempting to construct a model of the crystal structure of a polymer a principal requirement is that the chain structure must be compatible with the crystal structure into which the chains are packed. Thus, for a conjugated polymer, the rigid backbone and the requirement of invariance after translation by a lattice constant provide strict constraints on the possible chain directions in a unit cell.

With these constraints and with the use of the indices of poly(p-phenylene) as a guide, we are able to index the observed reflections by assuming two models:

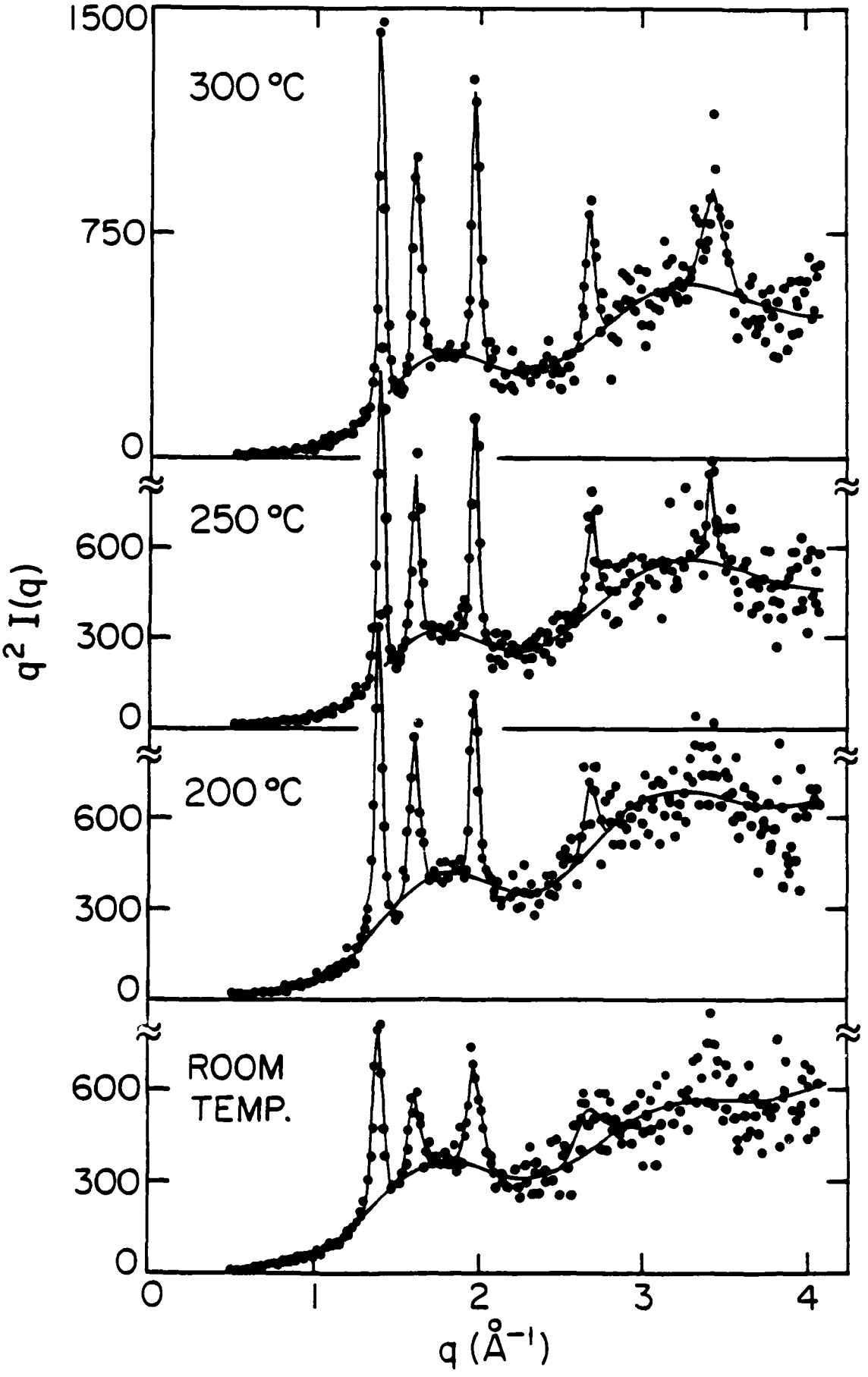
1500
750
0
300 °C
600
300
0
250 °C
600
300
0
200 °C
600
300
0
ROOM
TEMP.
0
1
2
3
4
q (Å⁻¹)
q² I(q)

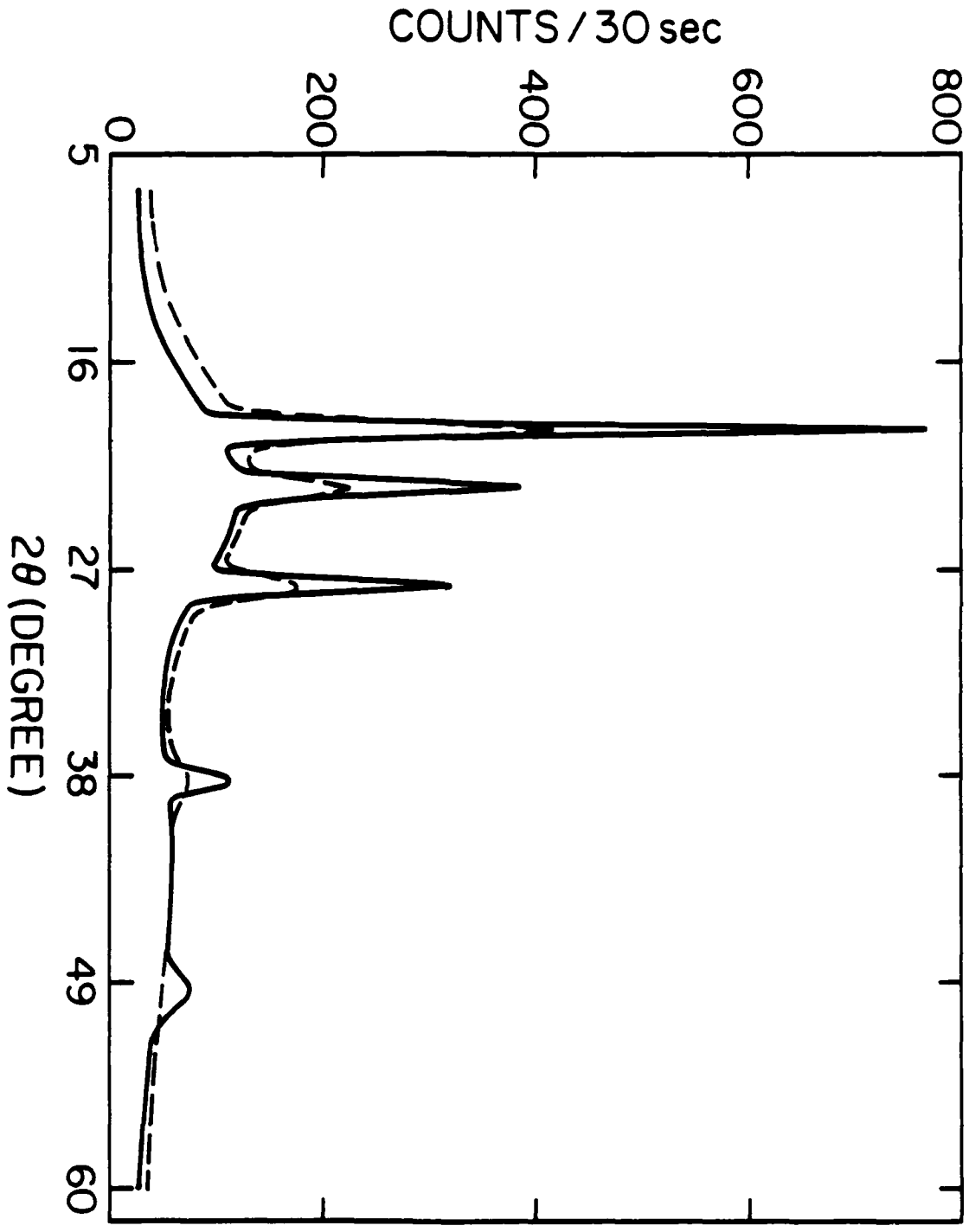
COUNTS / 30 sec
0
200
400
600
800
5
16
27
38
49
60
2θ (DEGREE)

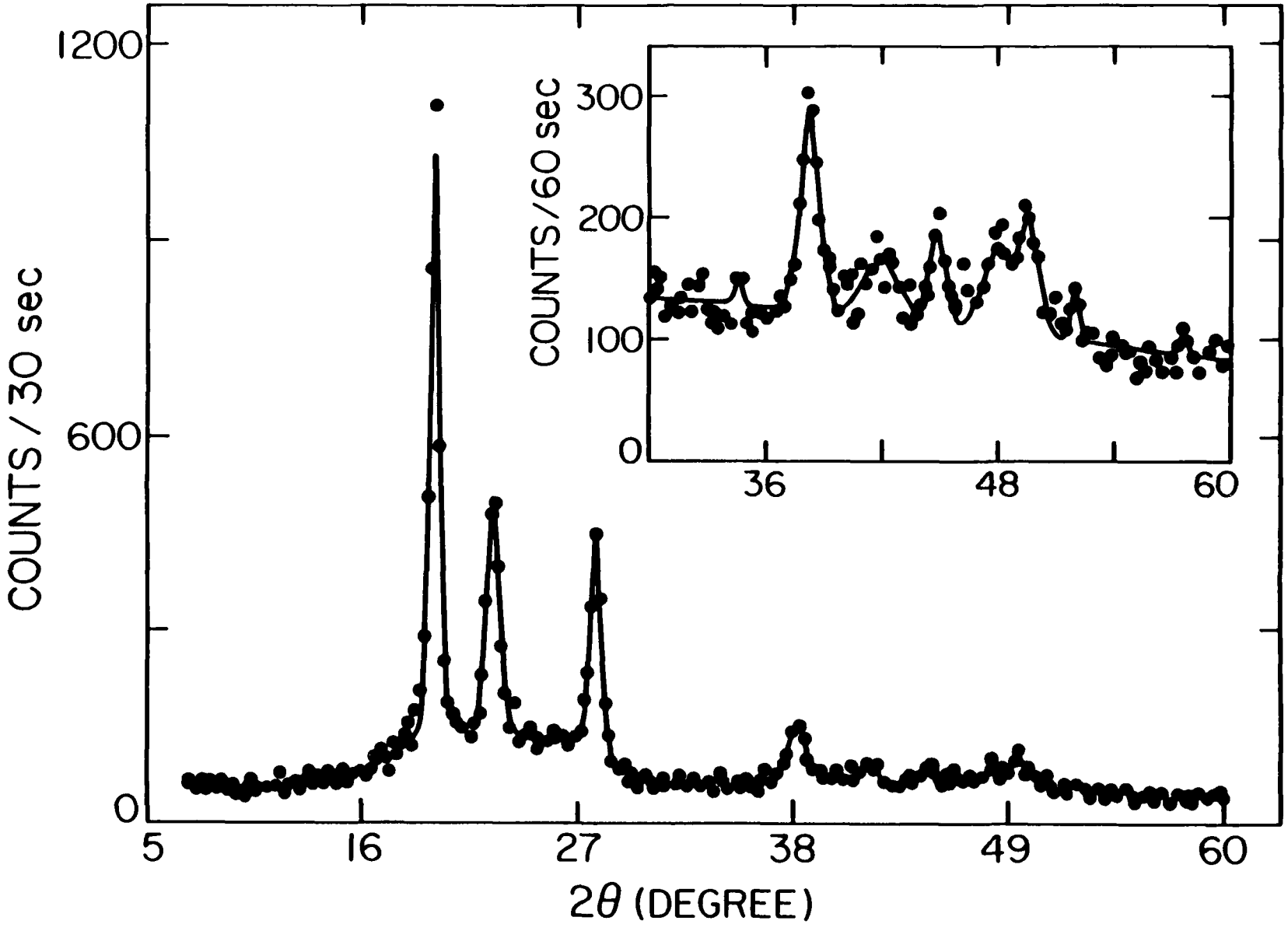
1200
600
0
COUNTS / 30 sec
5
16
27
38
49
60
2θ (DEGREE)
300
200
100
0
COUNTS/60 sec
36
48
60

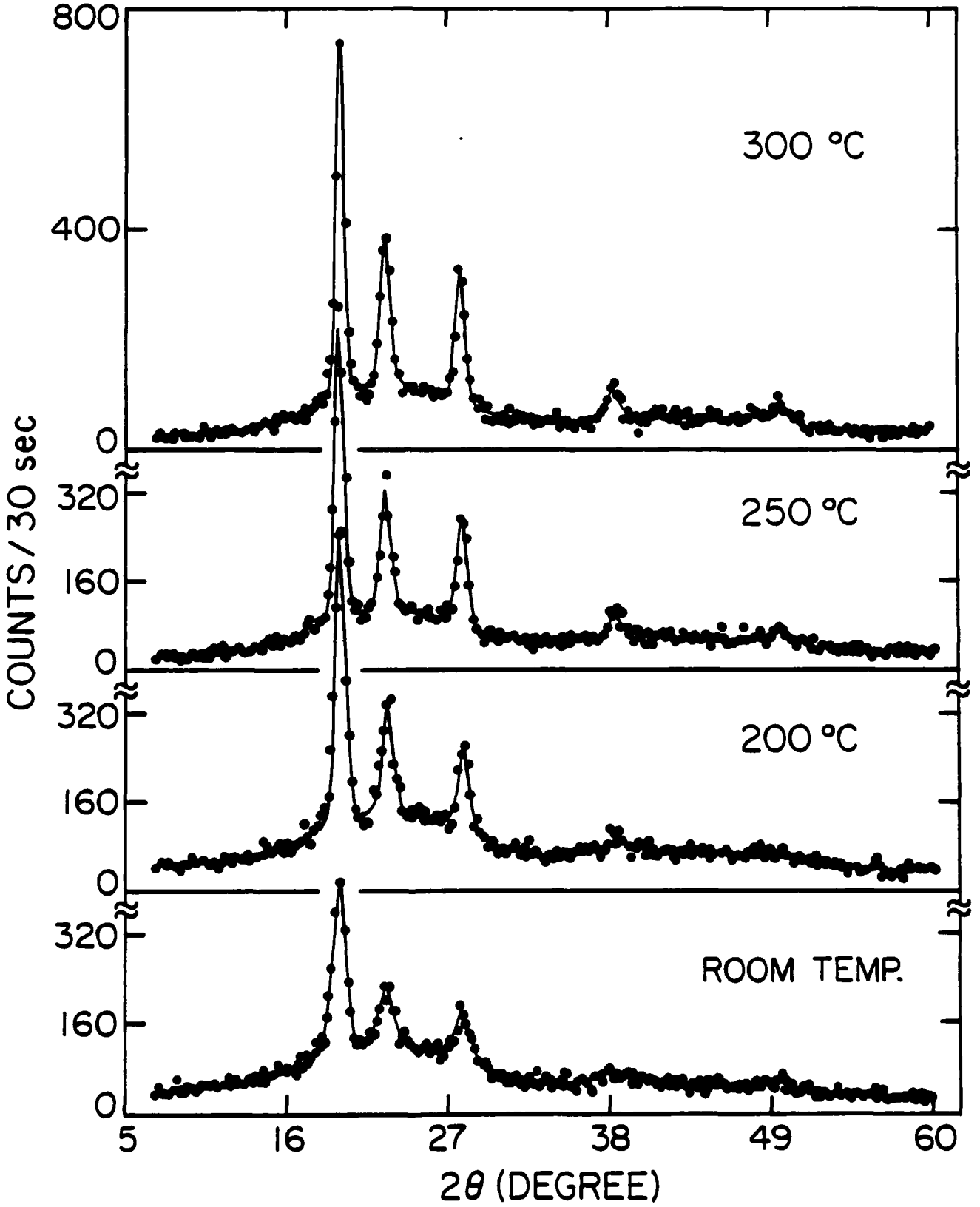
800
400
0
300 °C
320
160
0
250 °C
320
160
0
200 °C
320
160
0
ROOM TEMP.
COUNTS / 30 sec
5
16
27
38
49
60
2θ (DEGREE)

(a) 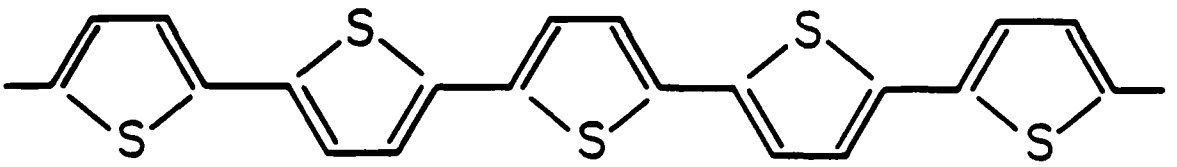

(b) 

FIGURE CAPTIONS

1 a. chemical structure diagram of polythiophene. b. two inequivalent structures for the thiophene heterocycle in polythiophene.

2a. X-ray powder diffraction curves for polythiophene after heat treatment at indicated temperatures for 30 minutes.

2b. X-ray powder diffraction curve for polythiophene after heat treatment at 380°C for 30 minutes.

3. Comparison of best fits to the scattering data of Fig. 2 from the as-synthesized material (dahsed curve) and from the same sample after annealing at 300°C for 30 minutes (solid curve).

4. X-ray powder diffraction intensity curve $q^2I(q)$, for polythiophene after heat treatment at indicated temperatures.

5. Comparison of best fits to $q^2I_{(q)}$ data of Fig. 4 from the as-synthesized sample and from the same sample after annealing at 300°C for 30 minutes.

6. Variation of X_{cr} in PT as a function of heat treatment temperature (in N_2).

7. Variation of coherence length (from the width of the most intense reflection, Table 2) as a function of the heat treatment temperature (annealed in N_2)

8. Thermogravimetric analysis (TGA) of polythiophene; solid curve solid curve - in N_2; dashed curve - in air.

Table 4 (continued)

b) Monoclinic Unit Cell

	2θ(°)	d,Å (observed)	d,Å (calculated)	Miller Indices	Poly(p-phenylene)[10] d,A	Miller indices
1.	19.73	4.500	4.520	110	4.525	110
2.	22.74	3.910	3.894	200	3.910	200
3.	27.98	3.189	3.187	210	3.190	210
4.	34.60	2.593*	2.614	120	2.600**	120
5.	38.28	2.351	2.351	310	2.354	310
6.	41.92	2.155*	2.162	$\bar{2}13$		
			2.166	$\bar{1}22$		
7.	44.98	2.015*	2.039	004	2.096	022
8.	48.24	1.887*	1.896	320	1.890**	320
9.	49.57	1.839	1.837	410	1.830**	410
10.	52.03	1.760*	1.767	$\bar{1}31$		
			1.755	$\bar{4}11$		
11.	57.60	1.600*	1.594	420	1.590**	420

$a=7.83\text{Å}$, 5.55Å, $c=8.20\text{Å}$, $\beta=96°$
$\rho=1.537$ g/cm^3

*very weak reflection observed on slow scans with 60 sec. per point

**very weak reflection (see ref. 10).

Table 4. X-ray Diffraction Data for Polythiophene

a) Orthorhombic Unit Cell

	2θ(°)	d,Å (observed)	d,Å (calculated)	Miller Indices	Poly(p-phenylene)[10] d,A	Miller indices
1.	19.73	4.500	4.522	110	4.525	110
2.	22.74	3.910	3.900	200	3.910	200
3.	27.98	3.189	3.191	210	3.190	210
4.	34.60	2.593*	2.614	120	2.600**	120
5.	38.28	2.351	2.354	310	2.354	310
6.	41.92	2.155*	2.176	221(213)		
7.	44.98	2.015*	2.008	004	2.096	002
8.	48.24	1.887*	1.897	320	1.890**	320
9.	49.57	1.839	1.840	410	1.830**	410
10.	52.03	1.760*	1.768	313		
			1.756	131		
			1.754	402		
11.	57.60	1.600*	1.595	420	1.590**	420

a=7.80Å, b=5.55Å, 8.03Å, β=90°
ρ=1.567 g/cm^3

Table 3. Crystallinity of PT as a function of k and integration interval (see eqn 5)*

RT

	$4\pi^2 k(\AA^2)$				
$q_2/2$	0	2	3	4	5
0.65	19.9	32.0	39.8	48.9	59.4
0.54	22.0	30.6	34.9	41.7	48.3
0.49	24.2	32.2	36.9	42.1	47.8
0.45	27.1	34.5	38.7	43.3	48.4
0.41	25.9	31.6	34.8	38.3	42.0
0.37	28.1	33.0	35.7	38.6	41.6
0.30	27.6	29.1	32.5	34.3	38.1
0.28	32.7	36.1	37.8	39.6	41.4
			36.5 (ave)		

250°C

	$4\pi^2 k(\AA^2)$				
$q_2/2$	0	2	3	4	5
0.65	23.0	37.1	46.1	56.7	68.9
0.54	25.3	35.2	41.2	48.0	55.5
049	28.8	38.2	43.8	50.0	56.8
0.45	23.6	42.7	47.9	53.6	59.9
0.41	34.4	42.0	46.3	50.8	55.8
0.37	38.7	45.4	49.2	53.1	57.3
0.30	37.8	42.7	44.5	47.0	49.5
0.28	44.3	48.7	51.0	53.5	56.0
			46.3 (ave)		

200°C

	$4\pi^2 k(\AA^2)$				
$q_2/2\pi$	0	2	3	4	5
0.65	20.9	33.7	41.9	51.5	62.6
0.54	23.2	32.4	37.9	44.1	51.1
0.49	26.1	34.7	39.7	45.3	51.5
0.45	30.1	38.2	42.9	48.1	53.6
0.41	31.1	37.9	41.8	45.9	50.4
0.37	34.5	40.5	43.8	47.3	51.0
0.30	36.3	40.5	42.7	45.1	47.5
0.28	42.7	47.0	49.2	51.5	54.0
			42.5 (ave)		

300°C

	$4\pi^2 k(\AA^2)$				
$q_2/2\pi$	0	2	3	4	5
0.65	28.7	46.2	57.5	70.7	85.9
0.54	29.1	40.6	47.5	55.3	64.0
0.49	31.6	42.0	48.1	54.9	62.4
0.45	36.4	46.3	52.0	58.2	60.0
0.41	37.1	45.2	50.0	54.7	60.8
0.37	41.1	48.2	52.2	56.3	54.8
0.30	41.8	46.7	49.3	52.0	61.8
0.28	48.9	53.8	56.4	59.1	67.6
			51.6 (ave)		

*$q_1/2\pi = 0.07$

Table 2. X-Ray data of PT powder; data on strongest crystalline reflection

Specimen treatment (in N_2)	2θ (degrees)	Corr. Height of peak	Half-width
1. room temp	19.65	300	0.96
2. 473°K, 30 min	19.64	520	0.82
3. 523°K, 30 min	19.63	525	0.73
4. 573°K, 30 min	19.62	671	0.66

Table 1. Chemical Composition of polythiophene (%)

Mol. wt.	C	H	S	I	Mg	Ni	
3958	56.71	2.63	37.05	3.17	49 ppm	51 ppm	(as-synthesized)
	58.67	2.40	39.24	0.13			(after anneal at 300°C)
98,700	58.43	2.45	38.99	0.13			calculated

References

1. M. Kobayashi, J. Chen, T.-C. Chung, F. Moraes, A.J. Heeger and F. Wudl, Synthetic Metals, 9 (1984), 77-86.

2a. A. Diaz, Chem. Scripta 17, 145 (1981).
b. G. Tourillon and F. Garnier, J. Electroanal. Chem. 135, 173 (1982).
c. T. Yamamoto, K. Sanechika, and A. Yamamoto, J. Polym. Sci., Polym. Lett. 18, 9 (1980).
d. J.W.-P. Lin, L.P. Dudek, J. Polym. Sci., Polym. Chem. edition 18, 2869 (1980).
e. C. Kossmehl and G. Chatzithedorou, Makromol. Chem. Rapid Commun. 2, 551 (1981).
f. J. Bargon, S. Mohmand, R.J. Waltman, IBM: Journal of Res. and Dev. 27, 330 (1983).
g. K. Kaneto, Y. Kohno, K. Yoshino and Y. Inuishi, J. Chem. Soc. Chem. Com. 382 (1983).

3. T.-C. Chung, J.H. Kaufman, A.J. Heeger and F. Wudl, Physical Reviews B 30 (2) (1983), 702-710.

4. H. Yoshida and N. Taneaki (private communication).

5. F. Moraes, H. Schaffer, M. Kobayashi, A.J. Heeger and F. Wuld, Phys. Rev. B 30, 2948 (1984).

6. F. Moraes, D. Davidov, M. Kobayashi, T.-C. Chung, J. Chen, A.J. Heeger and F. Wudl, Synthetic Metals (in press).

7. W. Ruland, Acta Cryst. 14, 1180 (1961); Polymer 5, 89 (1964).

8. T. Akaishi, K. Miyasaka, K. Ishikawa, H. Shirakawa and S. Ikeda, J. Polym. Sci., Polym. Phys. Ed. 18 (1980) 745-750.

9. X-Ray Diffraction Methods in Polymer Science, L.E. Alexander (Wiley Interscience, New York 1976); Chapter 7.

10. P. Kovacic, M.B. Feldman, J.P. Kovovacic and J.B. Lando, J. Appl. Polymer Sci., 12 1735 (1968).

11. J.L. Bredas, B. Themans, J.G. Fripiat, J.M. Andre and R.R. Chance, Phys. Rev B 29, 6761 (1984).

12. G.J. Visser, G.J. Heeres, J. Walters and A. Vos, Act Cryst B 24, 467 (1968).

VI. Conclusions

Heat treatment of polythiophene leads to a significant increase in the crystallinity and to improve coherence within the crystalline regions. The chain growth and extension is implied by the structural data and confirmed by chemical analysis. After annealing for 30 minutes at 300°C, the residual iodine content is consistent with growth of the polythiophene chains to approximately 1200 thiophene units, or a molecular weight of nearly 10^5.

Although the crystallographic data are incomplete, they do lead to an initial model of the structure of polythiophene. The results are consistent with an orthorhombic unit cell with lattice constants a=7.80Å, b=5.55Å and c=8.03Å or a monoclinic unit cell with a=7.83Å, b=5.55Å, c=8.20Å and $\beta = 96°$. In either case, the polymer axis is along c, and there are two polymer chains per unit cell. More detailed information on the chain packing and the precise determination of the monoclinic angle β will require a more detailed analysis based upon an enlarged data set from polythiophene of even higher crystallinity.

Acknowledgement: This study was principally supported by a grant from the Office of Naval Research. M. Kobayashi was supported by Showa Denko K.K. We *thank H. Yoshida of Showa Denko K.K. for sending us the preliminary powder* pattern results on polythiophene.

a) An orthorhombic unit cell with a = 7.80Å, b = 5.55Å, c = 8.03Å. The calculated and observed d-spacings (and the line indices) are given in Table 4a.

b) A monoclinic unit cell with a = 7.83Å, b = 5.55Å, c = 8.20Å and β = 96°. The calculated and observed d-spacings (and the line indices) are given in Table 4b.

Both Tables 4a and 4b list the d-spacings and indices for poly-(paraphenylene) for comparison. We note that dithiophene has a monoclinic structure[12] with lattice parameters a=7.76Å, b=5.90Å, c=8.91Å and = 106.6Å.

The value for c can be estimated from the known chemical structure of the thiophene monomer. Assuming 120° bond angles and standard carbon-carbon bond lengths for the pseudo-polyene backbone (see Fig. 1) the repeat unit is approximately 8.5Å. On the other hand, a repeat unit of approximately 7.8Å is obtained from analysis of the minimum energy configuration for quater-thiophene.[11] Thus, we conclude 7.8Å < c < 8.5Å, consistent with the values listed in Table 4.

With the above lattice parameters, the calculated density is approximately 1.55 g/cm^3 (see Table 4) assuming two chains per unit cell. The preliminary result of a density measurement (with no attempt to correct for porisity) of the as-synthesized is 1.21 g/cm^3 in satisfactory agreement with the calculation since the density of the partially amorphous material is expected to be less than that of the fully crystalline polymer. The measured density together with the crystallographic data does establish the existence of two chains per unit cell.

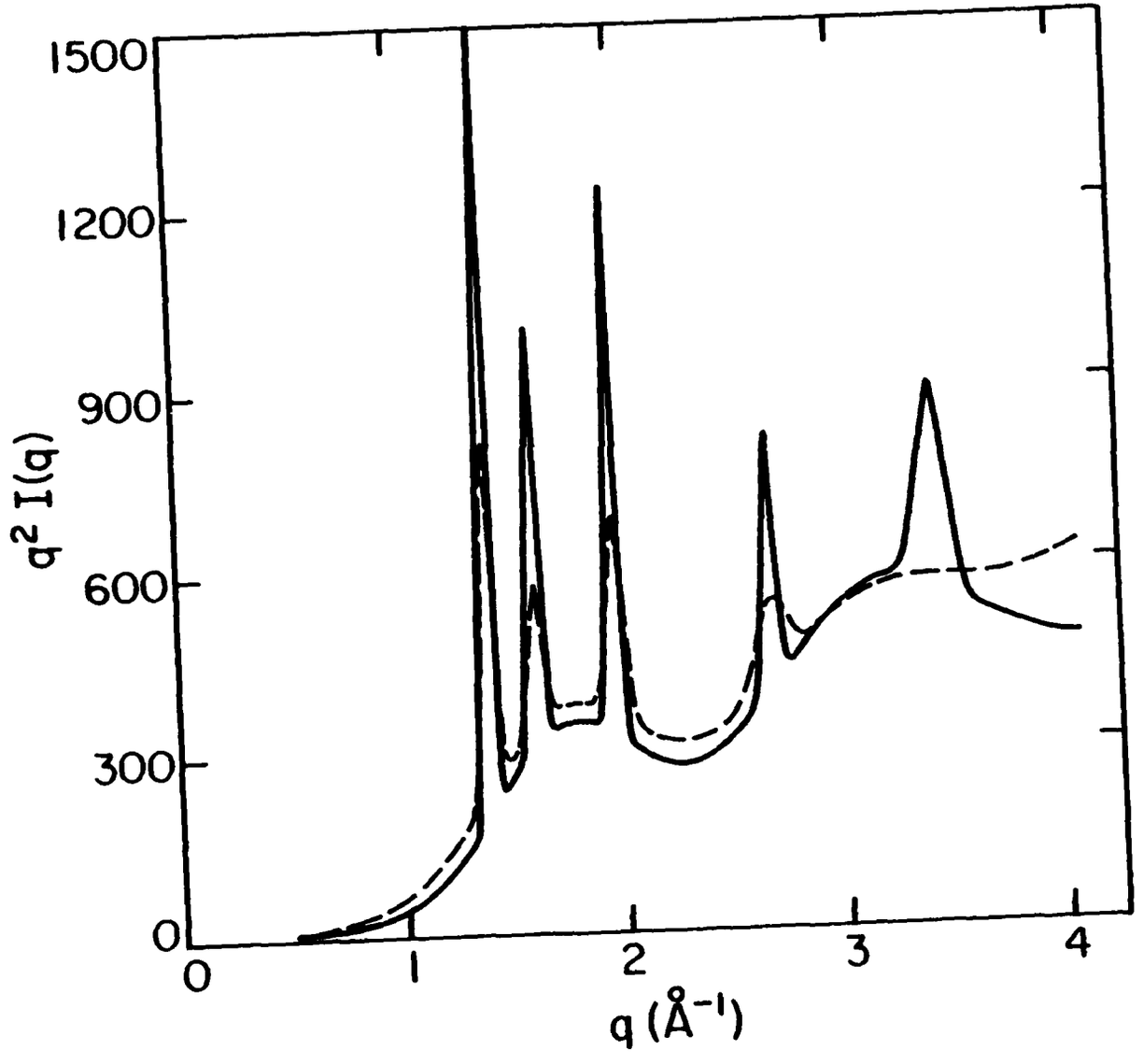
1500
1200
900
600
300
0
$q^2 I(q)$
0
1
2
3
4
q (Å^{-1})

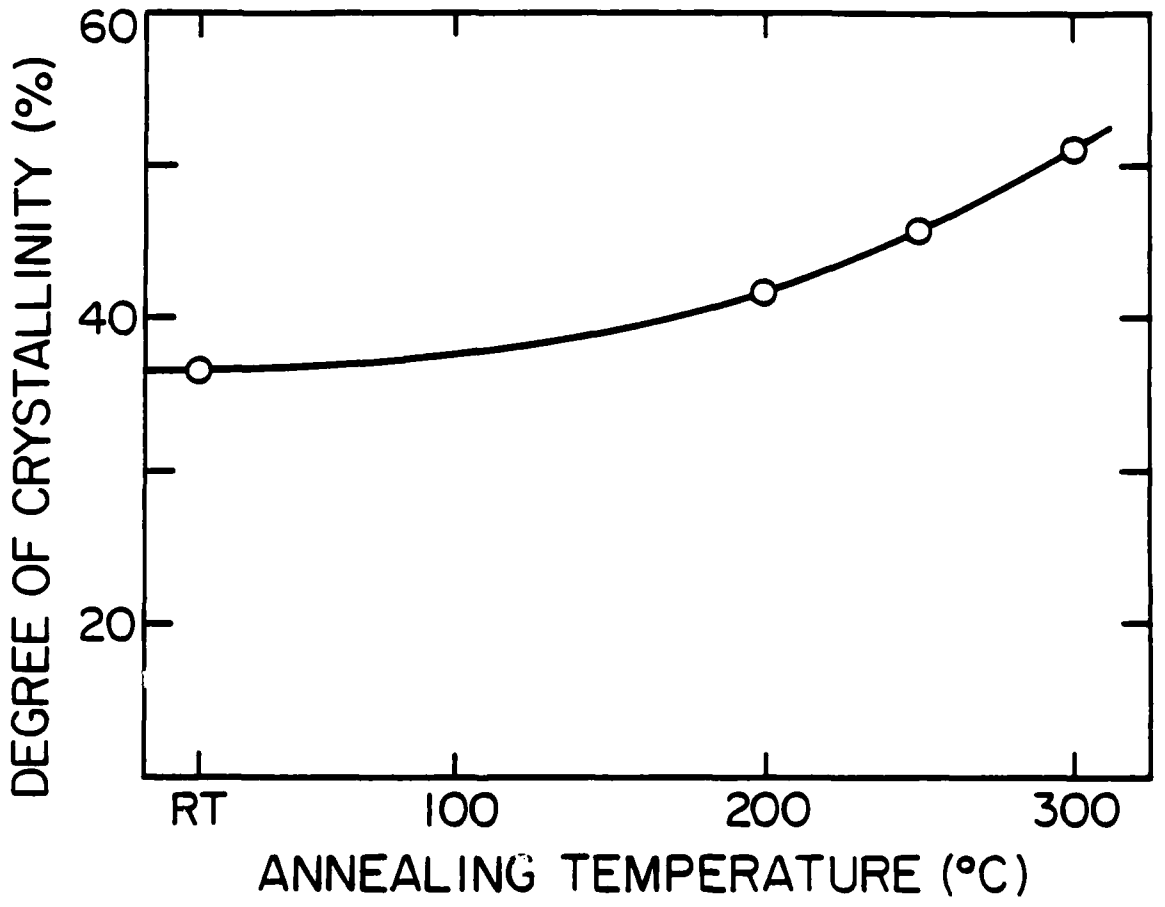
60
40
20
DEGREE OF CRYSTALLINITY (%)
RT
100
200
300
ANNEALING TEMPERATURE (°C)

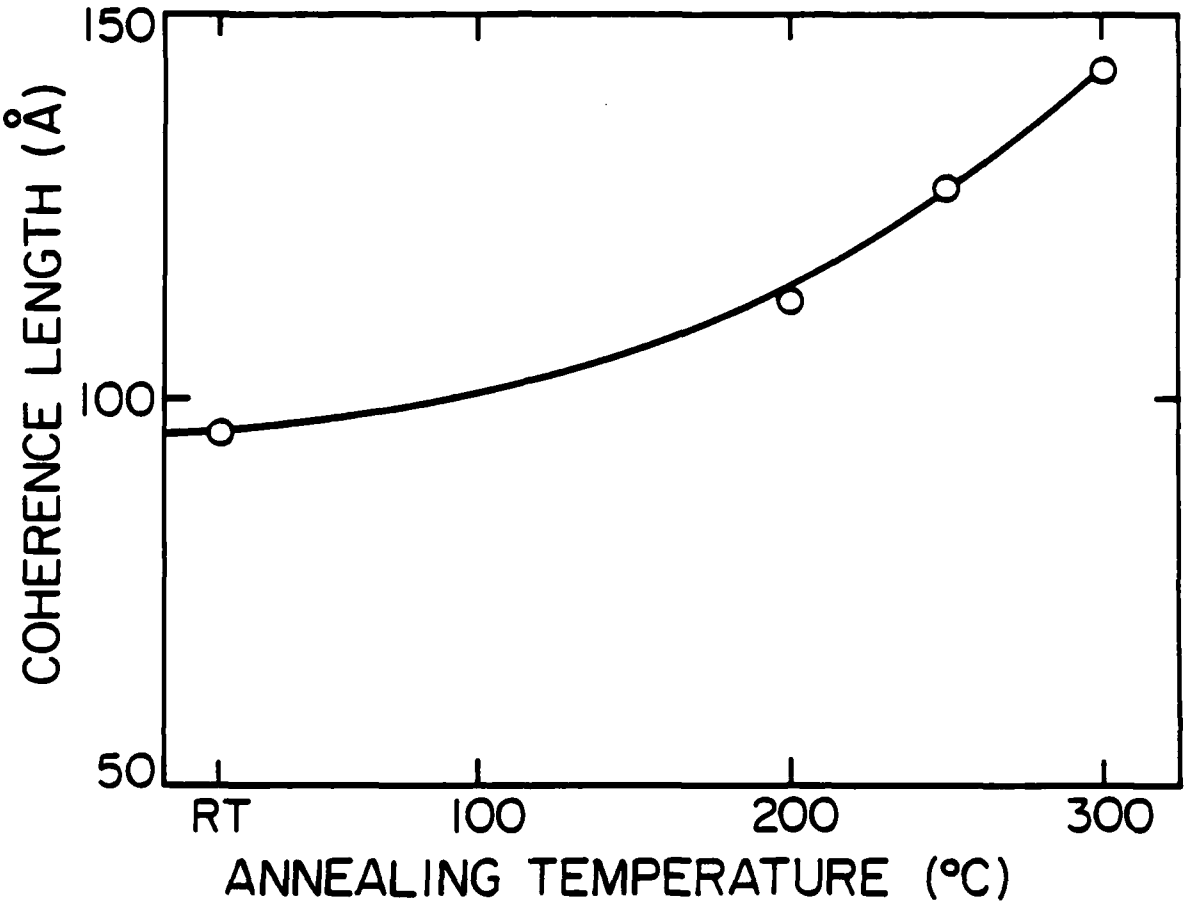
150
100
50
COHERENCE LENGTH (Å)
RT
100
200
300
ANNEALING TEMPERATURE (°C)

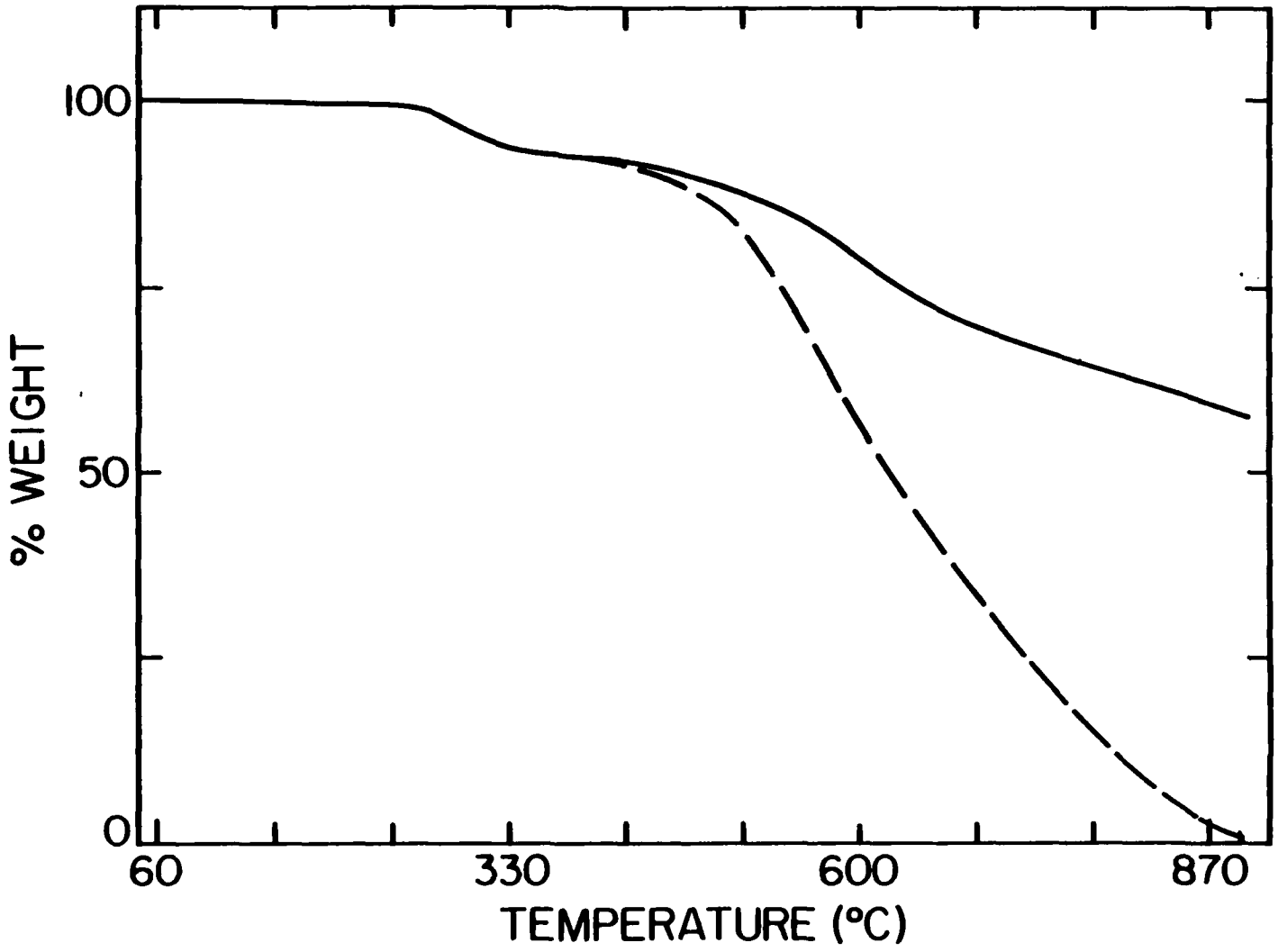
100
50
0
% WEIGHT
60
330
600
870
TEMPERATURE (°C)

END

FILMED

11-85

DTIC